Evaluating the Dynamics of Tension Mooring Supported Tidal Turbines

Song Fu*, Cameron Johnstone†
Energy Systems Research Unit
Department of Mechanical and Aerospace Engineering
University of Strathclyde
Glasgow, UK, G1 1XJ
song.fu@strath.ac.uk
cameron.johnstone@strath.ac.uk

***Abstract*—This paper reports the design of a tidal turbine station keeping system based on the adoption of a tensioned mooring system and investigates potential capabilities of introducing dampening into the system and the capabilities to reduce the peak loads tidal turbines experience during operations in high energy wave-current environments. A neutrally buoyant turbine is supported from a tensioned cable based mooring system, where tension is introduced by a buoy are fully submersed in water. The loading on the turbine rotor blades and buoy are calculated using a wave and current coupled BEMT. The modeling algorithm developed have been based on an inverted triple pendulum, responding to different sea state conditions in order to understand the response behavior of the system and the loads on blades in different flow conditions.**

Keywords:Tidal turbine, Mooring system, Modelling, Blade loads, Dynamics, Wave-current interaction

I. Introduction

The design of tidal turbine station keeping systems varies according to the different turbine architecture being considered and the method of attachment to the seabed being employed. Gravity base structures, drilled monopiles and drilled pin pile tripods are three widely applied support structures used today for tidal turbines. Moreover, flexible catenary mooring based systems are being adopted for the station keeping of floating tidal turbines.

In order to solve the tensioned mooring system, it is assumed to be a inverted triple pendulum system with external forces. A simple pendulum with external drive may oscillate periodically, quasi-periodically and chaotically [1, 2, 3]. A coupled pendulum with external drive are expected to experience more complicated dynamics. Existence of irregular vibrations and both periodic and chaotic trajectories of a mathematical double pendulum system is proven in [4]. The stabilization of inverted pendulums, which is highly nonlinear system has been extensively studied for control education and research purposes, however the moored turbine system are not as complex as other inverted pendulums due to the external forces are at specific axis and positions.

In this paper the tensioned mooring system is modeled as a special type of triple pendulum which is called a flail. Some researches was done by [5] for the flail system. The loading on the turbine rotor blades and buoy are calculated using a wave coupled blade element momentum theory (BEMT) code developed at the University of Strathclyde for the analysis of the turbine rotor-drive train analysis when operating in energetic wave-current flow conditions [6]. In addition, due to the turbine being able to move and respond to the moving flow field, the resulting motions due to flow field interactions should be taken into consideration.

II. Numerical model

In this context, a neutrally buoyant turbine is supported from a tensioned cable based mooring system, where tension is introduced by a buoy fully submersed in water, as shown in Figure 1.

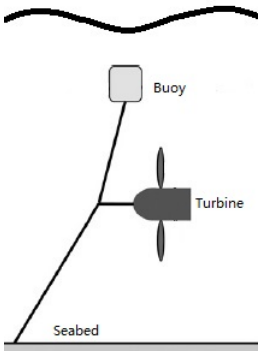

Fig. 1. Schematic of tensioned mooring turbine

The mooring lines are assumed to always be tensioned during operation. Therefore this system can be modelled as an inverted flail pendulum in order to calculate its dynamics, Figure 2 provides the model for the three elements in flail pendulum. Equations of motion of the pendulum system can be derived using Lagrange's equation

$$\frac{d}{dt}\left(\frac{\partial L}{\partial \dot{\theta}_i}\right) - \frac{\partial L}{\partial \theta_i} = Q_i \tag{1}$$

where $L = T - V$ is defined as the Lagrangian of the system, T is the kinetic energy and V the potential energy of system.

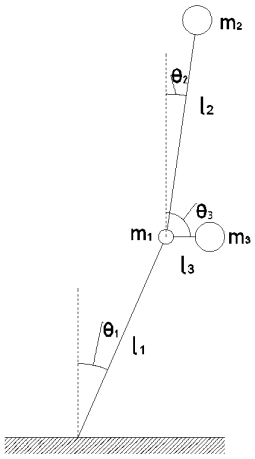

Fig. 2. The Schematic of "flail" pendulum

When there is no external force function Q_i, the Lagrangian of the system can be written as

$$\begin{aligned} L &= \frac{1}{2}(m_1+m_2+m_3)l_1^2\dot{\theta}_1^2 + \frac{1}{2}m_2l_2^2\dot{\theta}_2^2 + \frac{1}{2}m_3l_3^2\dot{\theta}_3^2 \\ &\quad + m_2l_1l_2\dot{\theta}_1\dot{\theta}_2\cos(\theta_1-\theta_2) + m_3l_1l_3\dot{\theta}_1\dot{\theta}_3\cos(\theta_1-\theta_3) \\ &\quad + (m_1+m_2+m_3)gl_1\cos\theta_1 \\ &\quad + m_2gl_2\cos\theta_2 + m_3gl_3\cos\theta_3 \end{aligned} \tag{2}$$

where m_1 is the lumped mass of three mooring lines at the connection node, m_2 represents the mass of buoy, m_3 represents the mass of the turbine. θ_1, θ_2 and θ_3 are generalized coordinates as shown in Figure 2.

It should be noticed that the turbine and the buoy are neutrally buoyant, so the potential energy terms in Equationn (2) can be eliminated. The new Lagrangian of the system becomes

$$\begin{aligned} L &= \frac{1}{2}(m_1+m_2+m_3)l_1^2\dot{\theta}_1^2 + \frac{1}{2}m_2l_2^2\dot{\theta}_2^2 \\ &\quad + m_2l_1l_2\dot{\theta}_1\dot{\theta}_2\cos(\theta_1-\theta_2) \\ &\quad + \frac{1}{2}m_3l_3^2\dot{\theta}_3^2 + m_3l_1l_3\dot{\theta}_1\dot{\theta}_3\cos(\theta_1-\theta_3) \end{aligned} \tag{3}$$

Substituting Equation (3) into Equation (1) yields the Euler-Lagrange differential equations of the system

$$\begin{aligned} (m_1+m_2+m_3)l_1^2\ddot{\theta}_1 + m_2l_1l_2\ddot{\theta}_2\cos(\theta_1-\theta_2) \\ + m_2l_1l_2\dot{\theta}_2^2\sin(\theta_1-\theta_2) + m_3l_1l_3\ddot{\theta}_3\cos(\theta_1-\theta_3) \\ + m_3l_1l_3\dot{\theta}_3^2\sin(\theta_1-\theta_3) \\ = Q_1 \end{aligned} \tag{4}$$

$$\begin{aligned} m_2l_2^2\ddot{\theta}_2 + m_2l_1l_2\ddot{\theta}_1\cos(\theta_1-\theta_2) \\ - m_2l_1l_2\dot{\theta}_1^2\sin(\theta_1-\theta_2) &= Q_2 \end{aligned} \tag{5}$$

$$\begin{aligned} m_3l_3^2\ddot{\theta}_3 + m_3l_1l_3\ddot{\theta}_1\cos(\theta_1-\theta_3) \\ - m_3l_1l_3\dot{\theta}_1^2\sin(\theta_1-\theta_3) &= Q_3 \end{aligned} \tag{6}$$

where Q_1, Q_2 and Q_3 are the generalized forces. In this case Q_3 is calculated from the turbine thrusts under wave-current coupled effect, Q_2 is from the buoyancy and wave-current coupled forces of the buoy, Q_1 will be obtained by the relation with Q_2 and Q_3.

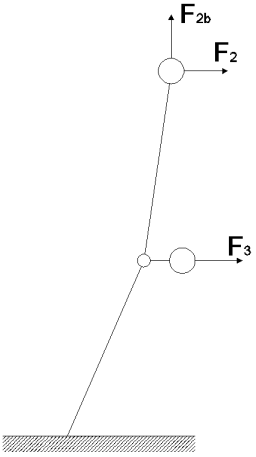

Fig. 3. Forces on the system

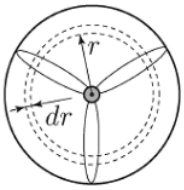

Fig. 4. Sectional area of turbine

Figure 3 shows the forcing conditions of the system. The momentum equations for thrust can be obtained by Blade Element Momentum Theory (BEMT) as

$$\mathrm{d}F_3 = 4\pi\rho\left[U^2a(1-a) + (b\Omega_\mathrm{r}r)^2\right]r\mathrm{d}r \tag{7}$$

where ρ is the water density, Ω_r is turbine angular velocity, a and b are the axial and angular induction factors obtained by the method [6]. In order to simply the calculation, the dynamic inflow effects is not employed in this model at present. The cross sectional area of $2\pi r\mathrm{d}r$ is as illustrated in Figure 4. Because the turbine is movable, a relative velocity U should be under consideration as

$$U = u - U_T \tag{8}$$

where U_T is the horizontal inertia velocity of the turbine itself which can be calculated as U_T=$\dot{\theta}_1l_1\cos\theta_1 + \dot{\theta}_3l_3\cos\theta_3$. u is the inflow velocity which is calculated by Linear wave theory

$$u = U_\infty + \frac{gHk}{2\omega(1 - U_\infty k/\omega)\cosh kh}\cosh k(h+z)\sin(kx - \omega t) \quad (9)$$

where U_∞ is the current speed which is considered as a constant in this paper, H is the wave height, ω is the wave angular frequency, k is the wave number, h is the water depth, x and z are the horizontal and vertical coordinates of the turbine which will also change with the operation time t as the turbine is movable.

The tip and hub loss correction factors [7, 8] is defined as

$$F_{\text{tip}} = \frac{2}{\pi}\cos^{-1}\left(\exp\left[-\frac{N}{2}\frac{(1-(r/R))}{(r/R)\sin\varphi}\right)\right) \quad (10)$$

$$F_{\text{hub}} = \frac{2}{\pi}\cos^{-1}\left(\exp\left[-\frac{N}{2}\frac{(r-R_{\text{hub}})}{r\sin\varphi}\right)\right) \quad (11)$$

where N is the number of blades, R is the rotor radius, R_{hub} is the radius of the turbine hub. φ gives as

$$\varphi = \tan^{-1}\left(\frac{U_\infty(1-a)}{\Omega_{\text{r}} r(1+b)}\right) \quad (12)$$

Included the loss correction Equation (10) becomes

$$\mathrm{d}F_3 = 4\pi\rho F_{\text{tip}} F_{\text{hub}}\left[U^2 a(1-a) + (b\Omega_{\text{r}} r)^2\right] r\mathrm{d}r \quad (13)$$

The buoy is assumed as a sphere, F_{2b} represents the net buoyancy of it, the drag force is written as

$$F_2 = \frac{1}{2}\rho v^2 C_D A \quad (14)$$

where C_D is the drag coefficient, A is the cross sectional area, v is the speed of the object relative to the fluid found as

$$v = u - U_B \quad (15)$$

where U_B is the horizontal inertia velocity of buoy as U_B=$\dot{\theta}_2 l_2\cos\theta_2 + \dot{\theta}_1 l_1\cos\theta_1$. The inflow velocity u can be calculated by Equation (8) with the coordinates of the buoy.

According to [9, 10], the generalized force can be obtained as

$$Q_k = \sum_{i=1}^{n} F_i \frac{\partial r_i}{\partial q_k} \quad (16)$$

where Q_k is the Generalized force associated with the k^{th} Eulaer-Lagrange differential equation, F_i is the external force, r_i is the position of the point of application and q_k is the generalized coordinate.

Thus, the generalize forces for this system are

$$Q_1 = F_3 l_1\cos\theta_1 - F_{2b} l_1\sin\theta_1 + F_2 l_1\cos\theta_1 \quad (17)$$

$$Q_2 = F_2 l_2\cos\theta_2 - F_{2b} l_2\sin\theta_2 \quad (18)$$

$$Q_3 = F_3 l_3\cos\theta_3 \quad (19)$$

When the generalized forces are obtained, the Euler-Lagrange differential equations of the system can be solved with given initial conditions.

III. Initial Conditions and System Parameters

In this study, two different sets of initial conditions are considered, which are shown in Table 1

TABLE I
INITIAL CONDITIONS

set 1	θ_1=0	$\dot{\theta}_1$=0	θ_2=0	$\dot{\theta}_2$=0	$\theta_3=\frac{\pi}{2}$	$\dot{\theta}_3$=0
set 2	θ_1=0	$\dot{\theta}_1$=0	θ_2=0	$\dot{\theta}_2$=0	$\theta_3=\frac{\pi}{3}$	$\dot{\theta}_3$=0

Angles in Table 1 are all measured in radian. Set 1 is the original condition that mooring lines l_1 and l_2 are at vertical position and l_3 is at horizontal position. In set 2, mooring line l_3 is not at horizontal position which means the naturally buoyant turbine is not adjusted to original position before operation.

The whole system has a lot of variables, this paper focuses on the primary ones which are external forces, and table 2 gives 6 external conditions, where regular and irregular waves are calculated from Joint North Sea Wave Observation Project (JONSWAP) spectrum [11]. The other parameters are given below

TABLE II
EXTERNAL DRIVE

	buoy radius	sea state	current speed
DLC 1	2 m	regular waves	1.5 m/s
DLC 2	3 m	regular waves	1.5 m/s
DLC 3	3 m	regular waves	2.5 m/s
DLC 4	2 m	irregular waves	1.5 m/s
DLC 5	3 m	irregular waves	1.5 m/s
DLC 6	3 m	irregular waves	2.5 m/s

$m_1 = 1$t $m_2 = 5$t $m_3 = 80$t $l_1 = 20$m $l_2 = 15$m $l_3 = 3$m $r = 10$m $h = 40$m $\Omega_r = 1.25$rad/s NRELs814

In this study, these parameters are set to be fixed in order to control the number of parameters.

IV. Results

In Barltrop [12] experiment, the 0.35m diameter turbine with NRELs814 blade profile was subject to regular waves with different heights and periods. Figure 5 shows three case from Barltrop experiment in order to verify the result obtained from the numerical model without dynamic wake formulation.

According to Figure 5, the flail model may not apply for the condition where the turbine is closed to the water surface, but

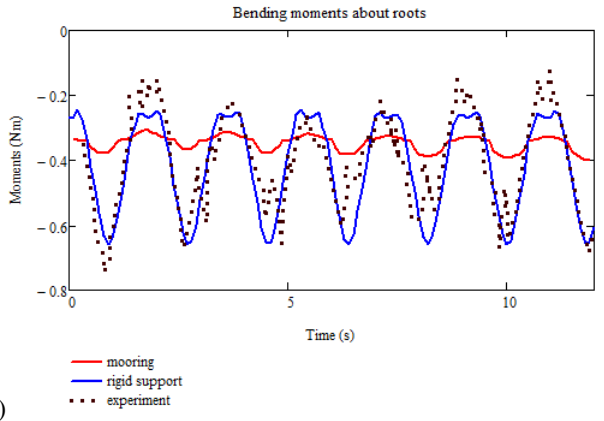

(a)

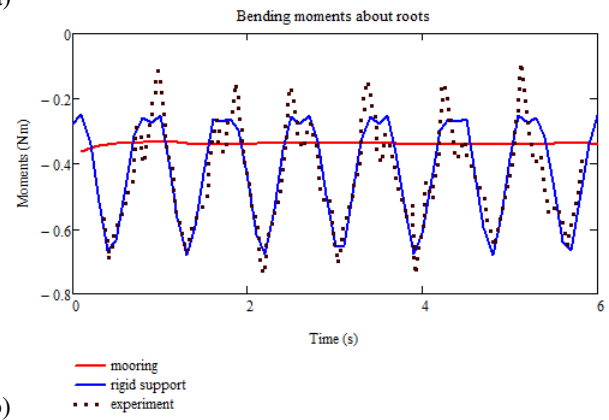

(b)

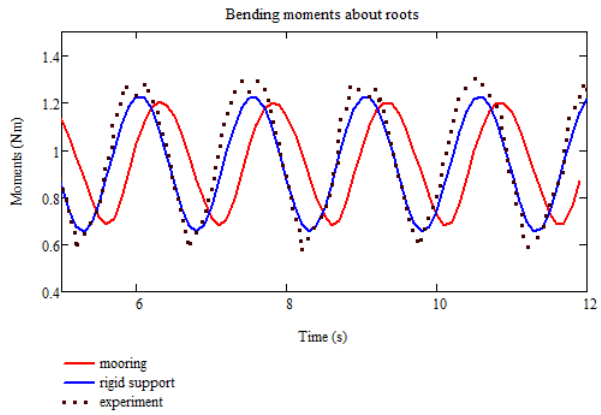

(c)

Fig. 5. (a) Numerical results and Barltrop experiment showing in-plane bending moments M_x in waves of 150 mm height and 0.5 Hz frequency and current speed of 0.3 m/s. (b) Numerical results and Barltrop experiment showing in-plane bending moments M_x in waves of 150 mm height and 1 Hz frequency and current speed of 0.3 m/s. (c) Numerical results and Barltrop experiment showing in-plane bending moments M_x in waves of 150 mm height and 0.5 Hz frequency and current speed of 1 m/s.

the model starts to work when moving the turbine away from the water surface. In this condition (c) the turbine is moved to a lower position to make the "flail" model work as the turbine operating in the shallow water, the results shows that in the shallow water the mooring system may not have advantages in blades forces reduction.

Figure 6 shows the trajectory of the system for one case during the simulation and the final positions of the system at 120s. In fact the motion of the buoy is relatively stable

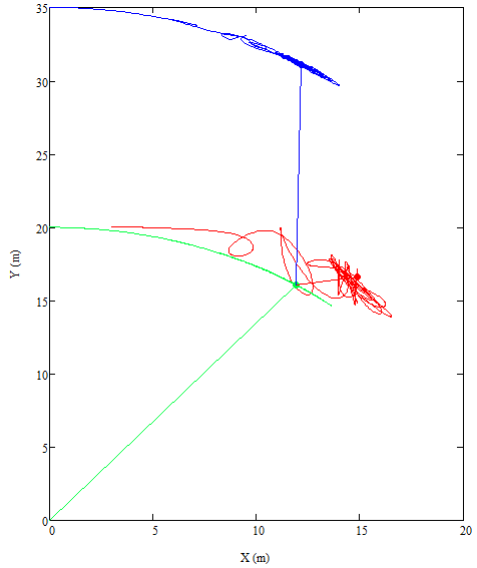

Fig. 6. Motion of the system at the end time

compared to the turbine, firstly the buoy moves alone an arc after it is driven by the external forces, then after several seconds it starts to slightly oscillate along a short section of the arc. Unlike the buoy, the oscillation of turbine can be observed clearly from Figure 6 and it is certain to affect the performance of the turbine during operation. In Figure 7, the displacementof the turbine is large at first, thus this paper will only focus on motions of the turbine from 10s to 120s.

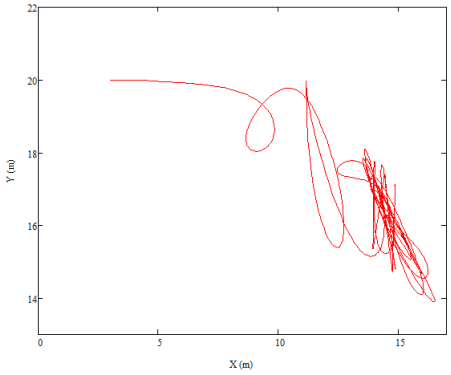

Fig. 7. Trajectory of turbine

A 2 minutes simulation is done for 7 different conditions in order to find out the effects of primary variables. It should be noticed that a output window from 10s to 120s is picked up because at the first 10s the motion of the system is much larger than the motion after 10s and the system approaches to normal operation. Table 3 gives the results for each case. Thrusts on blades for the tensioned mooring turbine during operation are compared with the rigid supported turbine, so that the wave influence on different supported turbines can be concluded. Moreover, the trajectory diagram and phase plane of the turbine gives the qualitative information about the dynamics of the turbine for each case.

TABLE III
RESULTS FOR 7 DIFFERENT CASES FROM 10S TO 120S

	Blades Thrusts Comparison	Trajectory Diagram of Turbine axes: x (m) - y (m)	Phase Plane of Turbine axes: $\theta_3(\mathrm{rad}) - \theta_3'(\mathrm{rad/s})$
Initial condition: Set 1 External drive: DLC 1	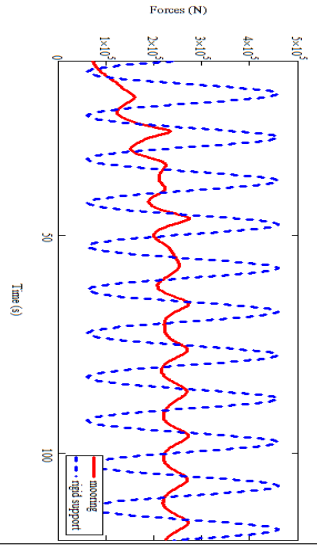	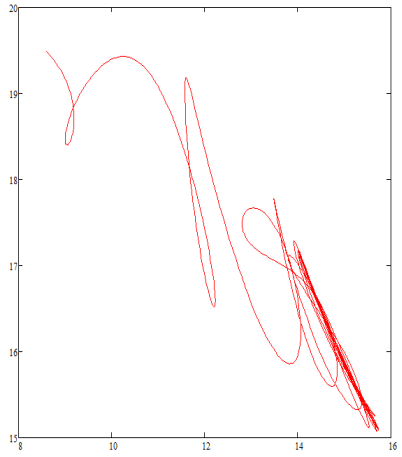	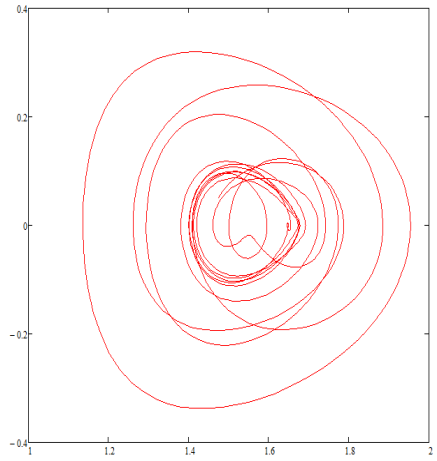
Initial condition: Set 1 External drive: DLC 2	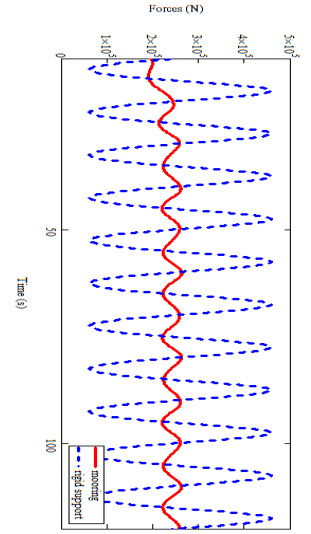	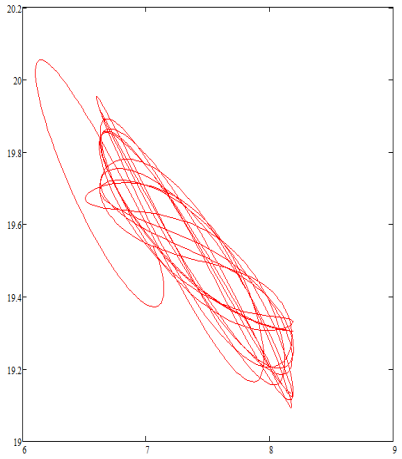	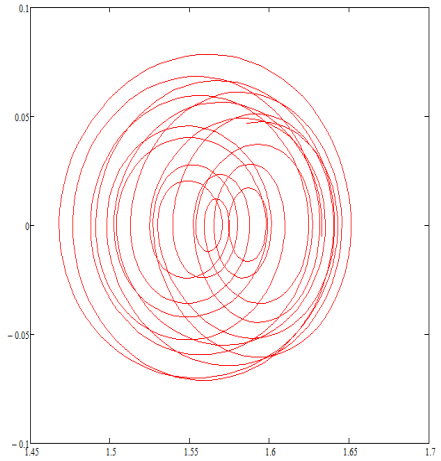
Initial condition: Set 1 External drive: DLC 3	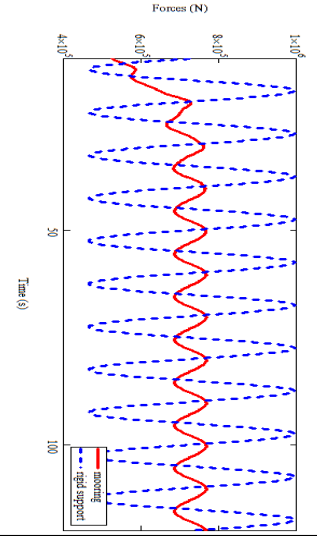	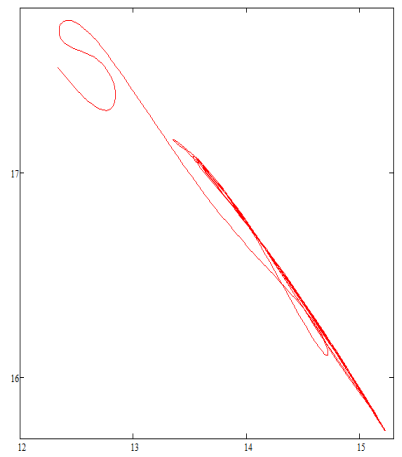	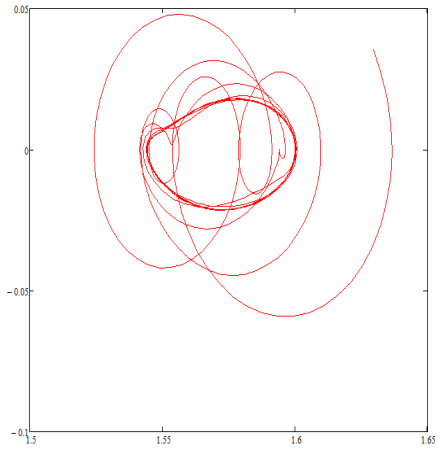

Initial condition: Set 1 External drive: DLC 4	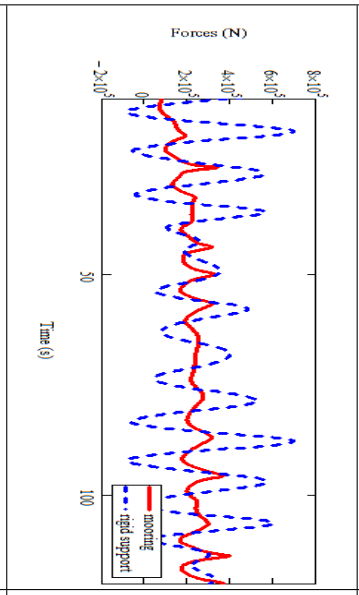	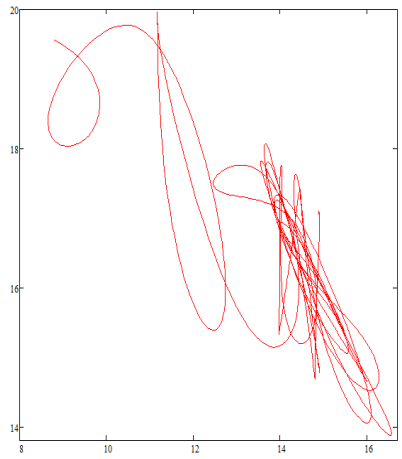	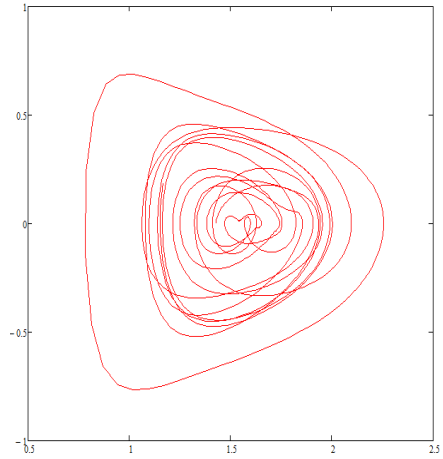
Initial condition: Set 1 External drive: DLC 5	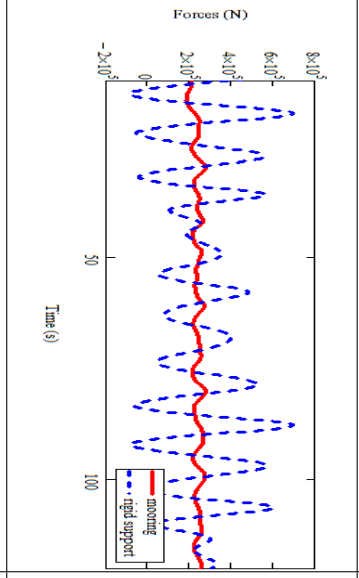	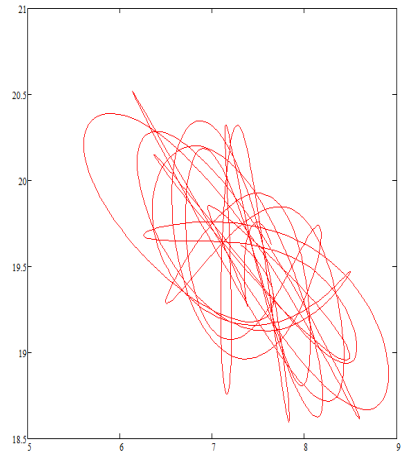	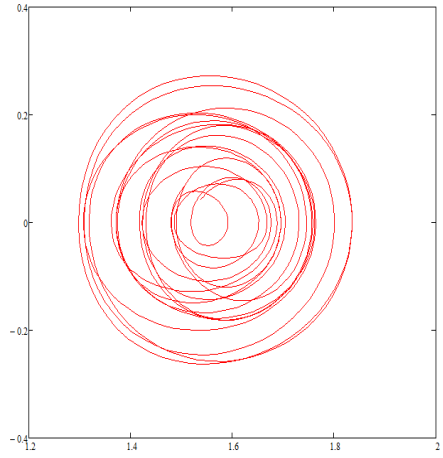
Initial condition: Set 1 External drive: DLC 6	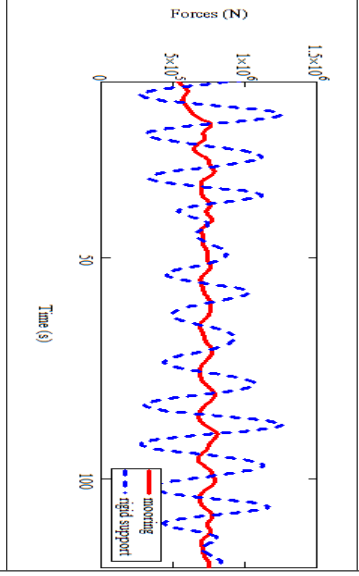	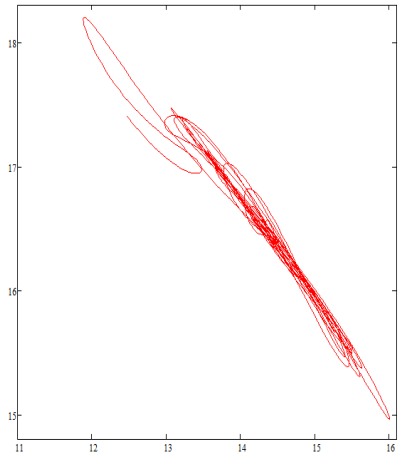	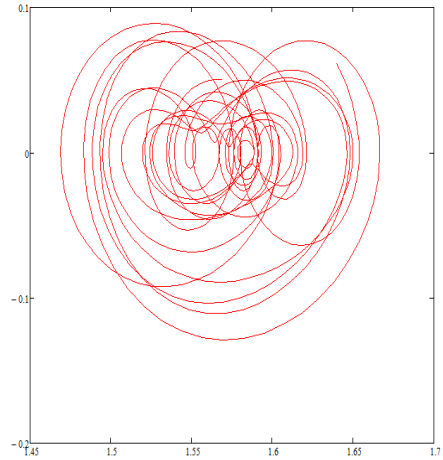

Initial condition: Set 2 External drive: DLC 6	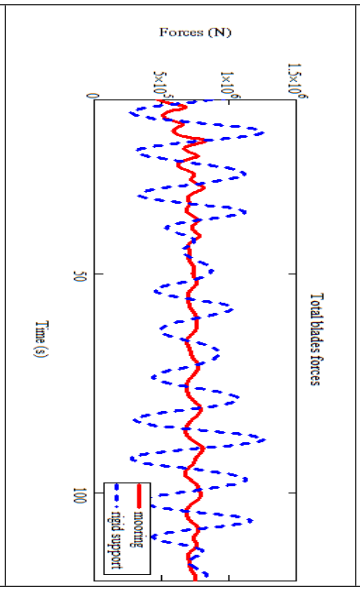	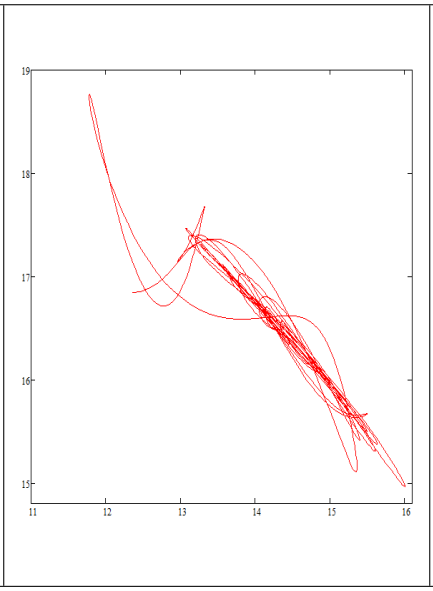	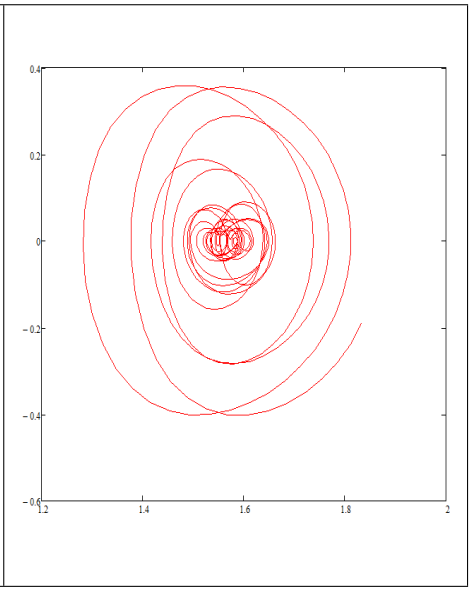

V. Discussions

According to Table 3, the blades thrusts comparison reveals that forces on mooring turbine blades are smaller and smoother than the rigid supported, which means the fatigue performance of mooring turbine will be better especially for irregular waves cases. DLC 1, DLC 3, DLC 4 and DLC 6 shows that the turbine will nearly move alone a short section of an arc, in regular waves as DLC 4 and DLC 6 the turbine is almost fixed to move on a track, which is an ideal operation environment. However, the DLC 2 and DLC 5 indicate that the buoy is a very important factor, when the buoyancy force which is reflected as the buoy radius is higher than a specific proportion of thrust (the ratio will be researched in the further research), the motion of turbine will not be stable, the turbine will oscillate around a central point as the trajectory diagram shows. Consider the attitude of turbine itself, the unstable motion may result in the pitch of turbine, so it is important to adjust the buoyancy according to the current velocities, a developed model will include the pitch of turbine as well. Furthermore, Set 1 and Set 2 have explained that the initial position of the turbine may not be a major factor for the system in a long period operation under the same external drive, both the phase plane and trajectory diagram will converge to a similar status after running for a moment. In addition, it is obvious that the irregular sea states will make the system more chaotic as it is shown in phase plane. In this paper the viscous force of the water is not under consideration, so the system is solved in integer-order model. However in order to make the model more reliable, it is necessary to solve the model in fractional-order [13, 14] which means the water damping term is added into the functions.

VI. Conclusions

The paper shows a fast simulation algorithm that is developed to model the neutrally buoyant turbine supported from a tensioned cable based mooring system.

A parametric study varing the initial conditions and external drives was undertaken in order to find out the major fators to the system. It showed that the buoy is a very important factor to the stability of the system.

Unlike rigid supported tidal turbines, the tensioned mooring supported tidal turbine investigated in this paper showed an obvious reduction of the forces on the blades due to there is a relative motion between the currents and the turbine. In irregular waves, the forces on the moored turbine blades will be smoother, this means a better performance in fatigue analysis.

References

[1] G. K. J. AWREJCEWICZ1 and C.-H. LAMARQUE, "Dynamics investigation of three coupled rods with a horizontal barrier," *Meccanica*, vol. 38, pp. 687–698, 2003.

[2] S. Bishop and M. Clifford, "Zones of chaotic behaviour in the parametrically excited pendulum," *J. Sound Vib.*, vol. 189, no. 1, pp. 255–267, 1996.

[3] A. Skeledon, "Dynamics of a parametrically excited double pendulum," *Physica D*, vol. 75, pp. 541–558, 1994.

[4] A. A. Martynyuk and N. V. Nikitina, "The theory of motion of a double mathematical pendulum," *International Applied Mechanics*, vol. 36, no. 9, pp. 1252–1258, 2000.

[5] W. S. Maria Przybylska, "Non-integrability of flail triple pendulum," *Chaos, Solitons & Fractals*, vol. 53, pp. 60–74, 2013.

[6] T. Nevalainen, C. Johnstone, and A. Grant, "A sensitivity analysis on tidal stream turbine loads caused by operational, geometric design and inflow parameters," *International Journal of Marine Energy*, 2016.

[7] R. M. Wen Zhong Shen and J. N. SÃÿrensen, "Tip loss corrections for wind turbine computations," *WIND ENERGY*, vol. 8, pp. 457–475, 2005.

[8] P. Moriarty, "Aerodyn theory manual," National Renewable Energy Laboratory, Tech. Rep., January 2005.

[9] I. O. Elmas Anli, "Classical and fractional-order analysis of the free and forced double pendulum," *Engineering*, vol. 2, pp. 935–949, 2010.

[10] P. R. A. Ohlhoff, "Forces in the double pendulum," *ZAMM - Journal of Applied Mathematics and Mechanics / Zeitschrift fÃijr Angewandte Mathematik und Mechanik*, vol. 80, no. 8, pp. 517–534, 2000.

[11] *Environmental conditions and environmental loads (DNV-RP-C205). Recommended practice*, Det Norske Veritas, 2007.

[12] A. G. D. C. N Barltrop, K S Varyani and X. Pham, "Wave-current interactions in marine current turbines," *Journal of Engineering for the Maritime Environment*, vol. 220, no. 4, pp. 195–203, 2006.

[13] M. Seredynska, "Nonlinear differential equations with fractional damping with applications to the 1dof and 2dof pendulum," *Acta Mechanica*, vol. 176, no. 3-4, pp. 169–183, 2005.

[14] I. M. F. R. S. Barbosa, J. A. T. Machado and J. K. Tar, "Dynamics of the fractional-order van der pol oscillator," in *Second IEEE International Conference on Computational Cybernetics*, 2004, pp. 373–378.